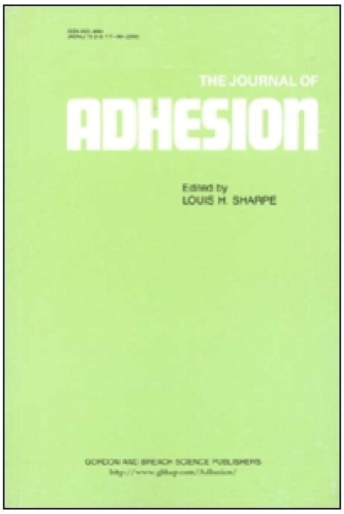

The Journal of Adhesion

Publication details, including instructions for authors and subscription information:
http://www.informaworld.com/smpp/title~content=t713453635

On Bridging and Mesogels

A. Halperin[a]
[a] CRPCSS, CNRS, Mulhouse, France

To cite this Article Halperin, A.(1996) 'On Bridging and Mesogels', The Journal of Adhesion, 58: 1, 1 — 13
To link to this Article: DOI: 10.1080/00218469608014396
URL: http://dx.doi.org/10.1080/00218469608014396

J. Adhesion, 1996, Vol. 58, pp. 1–13
Reprints available directly from the publisher
Photocopying permitted by license only

Amsterdam B.V. Published in The Netherlands
under license by Gordon and Breach Science
Publishers SA
Printed in Malaysia

On Bridging and Mesogels*

A. HALPERIN

CRPCSS, CNRS, 24 avenue du Président Kennedy, 68100 Mulhouse, France

(Received January 23, 1995; in final form July 7, 1995)

Copolymers bridging dissimilar domains are known to strengthen polymeric interfaces and to promote adhesion. A related effect gives rise to thermotropic elastomers formed by ABA triblock copolymers. Mesophases of ABA copolymers form physical networks due to bridging of different, glassy, A domains by B blocks. Shear alignment of the ABA melt produces "single crystal" mesonetworks with lamellar, cylindrical or micellar structure. The swelling of such mesonetworks by a selective solvent produces mesogels which differ from conventional gels because of their anisotropy and the high functionality of the cross links. Theoretical considerations concerning the bridging fraction, the swelling equilibrium and other issues are briefly reviewed for three types of systems: (1) Mesogels consisting of neutral, flexible ABA triblock copolymers. (2) Mesogels formed by ABA triblocks with a polyelectrolyte B block. (3) Mesogels produced by ABA triblock copolymers with a main chain liquid crystalline B block.

KEY WORDS: Mesogels; triblock copolymers; physical networks; bridging; swelling; polyelectrolytes; liquid crystalline polymers; adhesion.

I. INTRODUCTION

Bridging by polymer chains promotes adhesion with macromolecular materials. Compatilizers, such as block copolymers and random copolymers, are capable of strengthening interfaces in phase-separated polymer blends.[1] Grafted chains can enhance the adhesion between a solid and an elastomer.[2] These effects are attributed to interdigitation between the bridging chains and the polymeric material. The scope of bridging effects is actually wider. Another important manifestation is the formation of thermotropic elastomers from ABA triblock copolymers.[3] Thermotropic elastomers are physical networks formed in segregated ABA samples because some of the B blocks bridge different A domains. The A domains are typically glassy, thus making the physical bridges long lived. Note that the ABA triblock copolymers are capable of strengthening both AB interfaces and AA interfaces while the effectiveness of the AB diblocks is limited to AB interfaces. The study of bridging chains at AA interfaces is especially convenient in model systems based on thermotropic elastomers. This article is devoted to an elementary review of the theory of these model systems and the macroscopic signatures of the bridging chains.[4–13] The experimental route[14] to these model systems provides a good description of their essential features. One begins with a melt of ABA triblock copolymers. The temperature is then lowered below the threshold

---

* One of a Collection of papers honoring Jacques Schultz, the recipient in February 1995 of *The Adhesion Society Award for Excellence* in *Adhesion Science, Sponsored by 3M.*

of microphase separation. Thus, depending on the relative size of the blocks, one obtains lamellar, cylindrical or micellar mesophases. At this stage the melt is subjected to a shear treatment in order to align the mesophase so as to obtain a "single crystal" sample. The aligned mesophase is then quenched to below the glass transition temperature of the A domains. The result of this procedure is a physical network which retains the structure of the parent mesophase, thus we refer to it as a mesonetwork. Our discussion is mostly concerned with the properties of the mesogels obtained by swelling the mesonetworks by a selective solvent for the B chains, *i.e.*, a good solvent for the B blocks but a precpitant for the A blocks. Depending on the nature of the original mesophase one may obtain lammelar, cylindrical or micellar mesogels. The aligned lammelar mesogel consists of parallel glassy sheets of A polymer bridged by B chains. In the cylindrical mesogel the glassy A domains are cylindrical. Clearly, no alignment is necessary in the case of micellar mesogels where the glassy A domains are spherical. The study of mesogels allows access to a rich phenomenology traceable to the bridging chains; in particular, the swelling equilibrium, the deformation behaviour and their dependence on the solvent quality. As we shall discuss, this repertoire is even broader if one considers also polyelectrolyte and liquid crystalline B chains.

The interest in physical mesonetworks and mesogels is actually wider. As networks, these are distinctive because of their very high functionality and because of the strong anisotropy of the lamellar and cylindrical systems. This, in turn, leads to a distinctive anisotropic swelling behaviour of the corresponding mesogels. Furthermore, gel formation by ABA triblolck copolymers is probably the simplest example of physcal gelation and is, thus, an attractive model system from this perspective. The formation of mesonetworks is also a distinctive feature of triblock and multiblock copolymers. It is absent in diblock copolymers which otherwise exhibit essentially the same phase behaviour. This last point is of obvious relevance to polymer science where the study of block copolymers is of great current interest.[15] It is also of interest to surface science because of the close resemblance between diblock copolymers and monomeric amphiphiles. From this point of view the gel formation by ABA triblock copolymers is a distinctive feature of copolymeric surfactants. As a final point, these macroscopic systems are of interest because they incorporate grafted, or tethered, chains, i.e., chains attached to a surface by their head groups. This, too, is a topic attracting considerable current activity.[16] Mesogels allow for the study of tethered chains in macroscopic samples rather than in interfacial regions, as is the case in most other model systems.

The mesonetworks/mesogels considered in the following are formed by symmetric ABA triblock copolymers. The polymerisation degree of the two A blocks are identical and denoted by N_A. The nature of the mesophases is determined by the ratio $\alpha = N_B/2N_A$ where N_B is the polymerisation degree of the B blocks. Both N_A and N_B are much larger than unity. When $\alpha \approx 1$ the stable mesophase is lammelar. Cylindrial and micellar phases become dominant as α decreases. As indicated, the A blocks are flexible, neutral, isotropic chains with glass transition temperature, $T_g(A)$, above room temperature. The discussion concerns three families of systems, differing in the nature of the B blocks. In the simplest, reference, system and B blocks are flexible isotropic chains with $T_g(B)$ below room temperature, *i.e.*, the B domains are rubbery at the temperature range of interest. In the second system the B blocks are weak polyelectrolytes, *i.e.*, the B chains carry ionizable groups separated by m monomers such that $N_B \gg m \gg 1$. In the discussion it is assumed that the polyelectrolyte B blocks dissociate only in solvents of high dielectric constants such as water. Thus, in the melt state the B blocks are not dissociated and their behaviour is essentially indistinguishable from that of neutral flexible chains. As a result, the polyelectrolyte nature of the blocks will affect mostly the behaviour of the swollen mesogels while having little effect on the mesonetworks. In the third system the B blocks are main chain liquid crystalline polymer (LCP) blocks consisting of monomeric nematogenes joined by short, flexible spacer chains. For this system the discussion is confined to the case where the nematic-isotropic transition takes place above $T_g(A)$ but well into the microphase separated regime. Accordingly, the onset of nematic order is expected to affect both the properties of the mesonetwork and of the mesogel. The mesogels are obtained from the aligned mesonetworks by swelling with a selective solvent for the B blocks. In the second case, the selective solvent is assumed to be of high dielectric constant, *e.g.*, water. Nematic selective solvents are necessary to obtain the mesogels when the B blocks are LCP.

A complete description of the theory of mesogels is beyond the scope of this article. Instead, we present the meanfield free energies of certain types of mesogels and briefly discuss the necessary elaborations of this simple description. In other cases the discussion is entirely qualitative. A more complete analysis may be found in the quoted references. The equilibrium fraction of B chains is discussed in section II both for neutral flexible B blocks and for main chain LCP B blocks. Section III deals primarily with the swelling equilibrium of simple mesogels. Polyelectrolyte mesogels are discussed in section IV and the qualitative aspects of liquid crystalline mesogels are summarised in section V. Experimental studies and simulations are briefly mentioned in the final section.

II. THE EQUILIBRIUM BRIDGING FRACTION

One can envision a number of possible states of an ABA triblock in a mesonetwork. When both A blocks are embedded in the same a domain the B block forms a loop. A bridge occurs when the two A blocks inhabit different A domains. In principle, one should also allow for “dangling ends”, *i.e.*, triblocks with only one of the A blocks embedded in an A domain while the other is immersed in the B melt. However, our discussion focuses on the strong segregation limit where the AB interface is sharp and the associated surface free energy is high. In this limit the dangling ends population may be neglected. What is the fraction, q_{eq}, of bridging B chains in equilibrium? q_{eq} is determined by two factors:[5–7,11–13] The difference in the elastic free energy of loops and bridges and the mixing entropy of the two species. The free energies of loops and bridges differ because the configurational entropy of the bridges is lower. This can be understood as follows: The configurational entropy of the loops can be approximated, up to a ln N_B term, as that of two grafted chains obtained by cutting the loop into two equal parts. Each of the two halves has a free, unconstrained end which may be found anywhere within the layer. In marked contrast, each of the two ends of a bridging chain is constrained to a different AB boundary.

To quantify this argument it is necessary to resort to a SCF theory developed by Semenov.[17] In the otherwise powerful Alexander model[16,18] the two states are indistinguishable because all chains are assumed to be uniformly stretched. The details of the analysis are beyond the scope of our discussion. Nevertheless, insight may be gained by comparing an early but faulty approach of Zhulina and Halperin[5-7,11] with a recent, more accurate analysis of Matsen.[13] In the first approach, the bridging in an ABA lamella is considered analogous to the adsorption of a brush onto a surface which is attractive to the free ends. The midpoints correspond to the free ends in the adsorption problem, *i.e.*, each B block is cut into two equal parts. Within this picture, the lamellar midplane corresponds to the adsorbing surface. Each chain is allocated an area of Σ and the layer thickness is thus $N_B a^3/\Sigma$ where a is the characteristic size of a monomer. The SCF analysis of the adsorbing brush[19,20] suggests that the B layer consists of three regions. A central region, of thickness $2d$, comprised solely of uniformly-stretched bridging chains, and two boundary layers, of thickness h, incorporating both bridges and loops. In the bounary layers, the chain stretching varies with the distance from the surface, x. The average elastic free energy per chain at the boundary layer is

$$F_b/kT = (1-q)(3/2a^2)\int_0^h d\eta\, g(\eta)\int_0^\eta E_n(x,\eta)\,dx + q(3/2a^2)\int_0^h E_b(x,h)\,dx. \tag{1}$$

$E_n(x,\eta)$ is proportional to the local tension, $kT(3/2a^2)E_n$, in an ideal, non-bridging Gaussian chain whose free end is located at height η and $g(\eta)$ is the height distribution of the free ends. $E_b(x,h)$ is proportional to the local tension in a Gaussian segment of a bridging chain whose end is always located at height h. The elastic free energy per chain in the central region is

$$F_c/kT = 3q(H_o - h)^2/[2(N-N')a^2] \tag{2}$$

where $2N = N_B$ and N' is the number of monomers in the boundary layer. $H_o = Na^3/\Sigma$ is the thickness of the B half layer. By minimising $F_b + F_c$, subject to the appropriate constraints, one obtains the average elastic free energy per chain for a given q, $F_{eq}(q)$. In the limit of small q, $F_{el}(q)/kT = (F^o_{el}/kT)[1+(2q/\pi)^4]$ where $F^o_{el}/kT \approx H_o^2/Na^2$ is the elastic free energy per chain within the Alexander model, assuming uniform stretching. The equilibrium value of q is found by minimising

$$F_{\text{chain}}/kT = F_{el}(q)/kT + q\ln q + (1-q)\ln(1-q). \tag{3}$$

For small q this leads to $4(F^o_{el}/kT)(2\pi)^4 q^3 + \ln q = 0$ which may be solved numerically to yield the approximate scaling form $q_{eq} \approx (F^o_{el}/kT)^{-\beta}$ with $\beta \approx 1/4$. Altogether

$$q_{eq} \approx N^{1/4}a^{1/2}/H_o^{1/2} \sim \Sigma^{1/2} N_B^{-1/4}. \tag{4}$$

This result is actually asymptotically valid in the limit of very strong segregations, when Σ is very small.

The approach outlined above is faulty in two respects. One, bridging is due only to chains with midpoints at the midplane. The contribution of midpoints located elsewhere is neglected. Two, when this constraint is relaxed, it is important to use a more accurate expression for the mixing entropy.[13] In particular, to introduce a local mixing entropy density allowing for bridging due to midpoints off the midplane. The probability of finding a midpoint at altitude η is $g(\eta)$. The corresponding probability for a bridge is thus $P_B(\eta) \sim g(\eta)g(2H_o - \eta)$ while that of a loop is $P_L(\eta) \sim g^2(\eta)$. Altogether, the normalised probability densities are

$$P_B(\eta) = g(\eta)g(2H_o - \eta)/[g(\eta) + g(2H_o - \eta)] \tag{5}$$

$$P_L(\eta) = g^2(\eta)/[g(\eta) + g(2H_o - \eta)]. \tag{6}$$

The global mixing entropy is obtained by integration of the local mixing entropy as expressed in terms of $P_B(\eta)$ and $P_L(\eta)$. Because of this modification it is also necessary to consider the variation of the free energy functional with respect to $g(\eta)$, thus allowing for the different elastic penalties associated with the various bridging configurations. The three distict lammelar zones no longer appear within this analysis. Rather, the midpoints are distributed throughout the B layer. In the present context, the main conclusion of the Matsen analysis is that $q_{eq} \approx 0.4$ for realistic systems. It is not, however, clear whether this q_{eq} is actually attained because of kinetic reasons and because of the effect of shear alignment.

Our discussion thus far has been confined to the simplest possible system, with flexible, neutral B blocks which are nonmesogenic, *i.e.*, incapable of forming liquid crystalline phases. In the following we consider mesonetworks with mesogenic, thermotropic, main chain LCP B blocks. In particular, the discussion is concerned with the effect of the onset of nematic order on q_{eq}. When the temperature of the nematic-isotropic transition, T_{NI}, is lower than $T_g(A)$ no effect is possible since the vitrification of the A domains prevents equilibration. In the opposite case, $T_{NI} > T_g(A)$, q_{eq} is expected to increase significantly. This enhancement of q_{eq} is due to the weakening of the Gaussian elasticity of the LCP in a nematic medium. Before we discuss this effect, it is necessary to present a brief introduction to the configurational statistics of main chain LCPs.[21,22]

A main chain LCP in an isotropic medium may be described as a worm-like chain.[23] The chemical structure is smeared out and the chain is pictured as a line of constant length, L, endowed with a rigidiy ε. ε defines a persistence length, ζ, for which the elastic energy, ε/ζ, is comparable with the thermal energy, kT, *i.e.*, $\zeta \approx \varepsilon/kT$. For long chains, $L \gg \zeta$, the large scale configurational behaviour is that of a random walk of L/ζ steps of length ζ. The chain span is, thus, $R_o^2 \approx (L/\zeta)\zeta^2 = L\zeta$. In a nematic environment the chain experiences a molecular field due to the nematic order. This brings about a decrease in the step length, a feature which is only possible within the framework of the worm-like chain model. A unit length of the chain is assumed to experience a Maier-Saupe potential of the form $V(\theta) = a_n S P_2(\cos\theta)$ where S is the nematic order parameter, θ is the angle between the chain element and the director $\mathbf{n}$ and $P_2(\cos\theta)$ is a Legendre polynomial of the second order. a_n is a phenomenological coupling constant which, together with ε, specifies the behaviour of the chain in a nematic environment. Two new length scales emerge: (i) The deflection length, λ, specifies the scale on which the nematic energy $a_n S\lambda$ is comparable with the elastic energy ε/λ, that is, $\lambda \approx (\varepsilon/a_n S)^{1/2}$. (ii) The short length, l, is defined by comparing the nematic energy $a_n S l$ with the thermal energy kT, that is, $l \approx kT/a_n S$. λ replaces the persistence length, $\zeta > \lambda$, in characterising the decay of angular correlations within the chain. Because of the nematic field the LCP is, in effect, confined to a virtual conical capillary with reflecting walls. Since the chain is deflected inwards upon each encounter with the walls, the angular correlations decay faster. When the chain is not too long, it is fully extended along the **n** direction, *i.e.*, $R_{\parallel_o} \approx L$. Its dimensions in the perpendicular direction arise from a two-dimensional random walk of L/l steps of length l leading to $R_{\perp_o}^2 \approx (L/l)\, l^2 = Ll$. The lateral span retains this form even for long chains. However, $R_{\parallel_o}$ then obtains a qualitatively different form. The new ingredient is hairpin defects. These are abrupt reversals in the trajectory of the chain. Their presence allows the chains to sample more of their configurational phase space. It is, thus, entropically favoured. On the other hand, the bend region of the hairpin is unfavourably oriented with respect to the nematic field and is, accordingly, energetically penalised. The overall size of the hairpin, Δ_h, is of order λ. The energy of a single hairpin, allowing for the elastic and for the nematic contributions is roughly $U \approx \varepsilon/\Delta_h + a_n S \Delta_h$. Minimalisation with respect to Δ_h yields $\Delta_h \approx (\varepsilon/a_n S)^{1/2} \approx \lambda$ and a characteristic energy of order ε/λ, $U_h \approx (a_n S \varepsilon)^{1/2}$. Since the existence of hairpins is not due to chemical structure but to thermal exitation, their density obeys a Boltzman distribution: $n_o l/L \approx \exp(-U_h/kT)$ where n_o is the number of hairpins on an unperturbed LCP at equilibrium. Note that the linear density is defined in terms of the short length l. This is because l specifies the uncertainty in the spatial position of the hairpins with respect to the chain end, thus, defining an effective lattice constant.[24,25] The hairpins give rise to a one-dimensional random walk in the direction of **n**. The number of steps is n_o and the average step length is L/n_o. For $n_o \gg 1$ the chain span in the direction of **n** is, thus, given by $R_{\parallel_o}^2 \approx n_o (L/n_o)^2 = L^2/n_o = Ll \exp(U_h/kT)$ rather than $R_{\parallel_o} \approx L$. Altogether, the LCP emerges as an ellipsoid with a major axis $R_{\parallel_o}$, oriented with **n**, which is much larger than the minor axis $R_{\perp_o}$.

This brings us to the central point. The shape anisotropy is also reflected in the elastic behaviour of the LCP. The involvement of random walk components suggests a Gaussian elastic behaviour. For weak deformations this is indeed the case. However, the elasticity of the major axis is much softer.[24,26] Since $R_{\parallel_o} \gg R_{\perp_o}$, the compression and stretching penalities, $F_{el}(R_\parallel)/kT \approx R_{\parallel_o}^2/R_\parallel^2$ and $F_{el}(R_\parallel)/kT \approx R_\parallel^2/R_{\parallel_o}^2$, are much weaker than the corresponding penalties associated with $R_\perp$. Furthermore, the elasticity of the major axis is typically much weaker than that of the LCP in an isotropic medium. Since $L/n_o \gg \zeta$, $R_{\parallel_o}^2 \approx L^2/n_o \gg R_o^2 \approx L\zeta$ and $F_{el}(R_\parallel)/kT \approx R_\parallel^2/R_{\parallel_o}^2$ is weaker than $F_{el}(R)/kT \approx R^2/L\zeta$. The corresponding elastic free energy density, f_{el}, is also modified. For flexible isotropic chains $F_{el} = a^{-2}(dr/dn)^2$, where n is the position along the chain trajectory, irrespective of direction. This form of f_{el} has been used to obtain q_{eq} of the nonmesogenic chains. However, for long main chain LCPs in the nematic state $f_{el}(R_\parallel)$ is of the form $f_{el}/kT = (al)^{-1} \exp(-U_h/kT)(dr_\parallel/dn)^2$. Consequently, the factor $(3/2a^2)$ in the relevant equations is replaced by $(3/2al)\exp(-U_h/kT)$. As a result,[9] $q_{eq} \approx (R_{\parallel_o}/H_o)^{1/2} \sim \Sigma^{1/2} N^{-1/4} \exp(U_h/4kT)$. Essentially, the bridging fraction below T_{NI} is larger by $\exp(U_h/4kT)$ because the Gaussian elasticity in this regime, which is due to the rearrangement of the hairpin defects, is much weaker.

III. SIMPLE MESOGELS

The preceeding section was devoted to mesonetworks above $T_g(A)$. In this temperature range neither the A nor the B domains are glassy. Consequently, the distribution of bridges and loops may, in principle, reach equilibrium. In the following, we consider the swelling of mesonetworks below $T_g(A)$. Mesogels are produced by swelling the aligned, single crystal mesonetwork by a selective solvent, *i.e.*, a good solvent for the B blocks but a precipitant for the A chains. Because $T < T_g(A)$ the swelling does not affect the A domains. Their dimensions and geometry remain unchanged. In particular, there is no effect on the area per chain, Σ, the thickness of the A domain and the fraction of bridging chains, q. In the following, we will consider the swelling equilibrium for the idealised case of $q = 1$, *i.e.*, when all B blocks form bridges.

The elementary units of the swollen mesogels are "brushes" of various geometries. The term refers to chains which are terminally anchored, grafted, to a planar surface, to a cylinder or to a sphere.[16] The grafting density is high so that the chains crowd each other, thus leading to chain stretching along the normal to the grafting surface. The swelling of the mesogels and of these elementary units is simply related in terms of a so called c^* theorem.[27] This equates the volume fraction of A monomers in the A domains of the mesogel to ϕ in the corona of the isolated unit. Thus, a swollen lamellar gel at equilibrium attains the dimensions corresponding to close packing of planar brushes at grazing contact, *i.e.*, at c^* of the lamellae. Accordingly, the theory of the swelling equilibrium of mesogels reduces to the theory of swollen brushes. To abbreviate the discussion further, we present a simplified version of this theory, incorporating Flory exponents. The chains are assumed to be Gaussian and the number of binary contacts is taken to scale as ϕ^2. This approximation ignores the effect of correlations, thus leading to an overestimate of both chain elasticity and the monomer-monomer interactions.[27] Nevertheless, the essential physical picture is correct. Furthermore, due to cancellation of errors, this approach does yield the correct dimension of the swollen brushes.

The primary features of a swollen planar brush are easily obtained within the framework of the Alexander model.[16,18] This Flory-type approach is based on two assumptions: (i) The monomer volume fraction within a layer of thickness H is constant, $\phi \approx Na^3/\Sigma H$. (ii) All chains are uniformly stretched with their ends straddling the layer boundary at height H. This model is actually strictly applicable to the case of a lamellar mesogel with $q = 1$. The swelling of the layer is favoured by repulsive monomer-monomer interactions. As H increases, ϕ decreases and with it the number of binary contacts. The swelling is arrested by the elasticity of the polymers since an increase in H is attained by stretching the chains. To quantify this argument, we express the free energy per chain of a brush immersed in a good solvent as

$$F_{\text{chain}}/kT \approx H^2/Na^2 + v\phi^2\Sigma H/a^3 \approx H^2/Na^2 + vN^2a^3/\Sigma H \tag{7}$$

where v is a dimensionless excluded volume parameter. The first term allows for the global Gaussian penalty associated with the chain stretching. The interaction free energy of the chain is reflected in the second term. Minimisation with respect to H yields the equilibrium thickness of the layer,

$$H_{eq}/a \approx N(a^2/\Sigma)^{1/3}. \tag{8}$$

The Alexander model is easily generalised to spherical and cylindrical geometries. In these situations, as in the case of the planar brush, it yields the correct scaling behaviour for the thickness of the layer. Such is the result for the Flory exponents as well as for the excluded volume, "scaling" exponents. However, while the discussion of the planar,

$q = 1$, layer allows for most of the relevant physics, the treatment of the non-planar geometries overlooks an important issue. The problem is as follows: For both spherical and cylindrical brushes, the volume available to the chain increases with the radius, r. Consequently, the chain crowding diminishes as r grows. Thus, one expects both ϕ and the chain stretching to decrease as r increases. Both effects are, however, prohibited within the framework of the Alexander model where ϕ and the chain stretching are assumed to be constant. A proper description of this effect, using the blob picture, has been developed following the pioneering work of Daoud and Cotton[28] as reviewed in Reference 16. The following discussion, after a recent presentation of Zhulina,[7,29] deals wtih the generalisation of the Alexander model with Flory exponents. In it, the chain ends still straddle the exterior boundary of the brush, however ϕ and the chain stretching are allowed to vary with r. Focusing on the good solvent behaviour, the free energy per chain consists of two terms. The elastic free energy of the chain is

$$F_{el}/kT = (3/2a^2)\int_R^{R+H} (dr/dn)\,dr \approx (aR^{d-1}/\Sigma)\int_R^{R+H} \phi^{-1} r^{1-d}\,dr. \tag{9}$$

The linar elastic free energy density, $(dr/dn)^2 dn$ may be written as $(dr/dn)\,dr$ when the chains are strongly stretched in the radial direction. When $\phi(r)$ is a slowly varying function, the increment of the total number of monomers is $dn_T \approx a^{-3}\phi(r)r^{d-1}dr$ where d, the dimensionality of the system, is $d = 1$ in the planar case, $d = 2$ for the cylindrical brush and $d = 3$ for the spherical one. The monomer increment per chain is $dn \approx (\Sigma/R^{d-1})dn_T$ where R is the radius of the grafting surface and R^{d-1}/Σ is the number of grafted chains. This leads of $dr/dn = a^3(R^{d-1}/\Sigma)\phi^{-1}r^{1-d}$ and to the final expression for F_{el}. The interaction free energy density due to binary monomer-monomer interactions is $a^{-3}vkT\phi^2(r)$ where v is the dimensionless second virial coefficient. The free energy density per chain is $(\Sigma/R^{d-1})a^{-3}vkT\phi^2$ and the interaction free energy per chain is, thus,

$$F_{\text{int}}/kT \approx (\Sigma/a^3R^{d-1})\int_R^{R+H} v\phi(r)^2 r^{d-1}\,dr. \tag{10}$$

The equilibrium characterstics of the brush are obtained by minimisation of $F_{\text{chain}} = F_{el} + F_{\text{int}}$ subject to the constraint of monomer conservation, *i.e.*,

$$(\Sigma/a^3R^{d-1})\int_R^{R+H} \phi(r)r^{d-1}\,dr = N. \tag{11}$$

The minimum condition, $-(R^{d-1}a/\Sigma)(\phi r^{d-1})^{-2} + (\Sigma/a^3R^{d-1})(v\phi + \lambda) = 0$, leads to the scaling form

$$\phi(r) = v^{-1/3}(R^{d-1}a^{3-d}/\Sigma)^{2/3}(a/r)^{2(d-1)/3}. \tag{12}$$

H_{eq} is determined by the constraint, Eq. (11), leading, for $H \gg R$, to

$$H_{eq}/a \approx (va^{3-d}R^{d-1}/\Sigma)^{1/(d+2)}N^{3/(d+2)}. \tag{13}$$

The average monomer volume fraction $\langle\phi\rangle \approx Na^3/H^d$ is

$$\langle\phi\rangle \approx c^{-d/(d+2)}(a^{3-d}R^{d-1}/\Sigma)^{2/(d+1)}N^{2(1-d)/(d+2)}. \tag{14}$$

Somewhat different forms are obtained for θ solvents, in which $v = 0$ and the interaction term reflects ternary monomer-monomer contacts leading to a free energy density of the form $w\phi^3$ where wa^3 is the third virial coefficient. In this regime, the swelling is weaker and, thus, H_{eq} is smaller while $\langle\phi\rangle$ is larger.

The swelling behaviour of single crystal mesogels approaches that of simple gels as their dimensionality grows, *i.e.*, along the sequence lamellar to cylindrical to micellar. The swelling is unidirectional in lamellar mesogels and bi-directional in cylindrical ones. In micellar gels, as in simple gels, the swelling is isotropic. $\langle\phi\rangle$ exhibits a similar trend, scaling, respectively, as N^0, $N^{-1/2}$ and $N^{-4/5}$ where $N^{-4/5}$ is the N dependence expected from simple gels. For comparison with polyelectrolyte gels note that different scaling laws characterise the equilibrium H_{eq} of the different mesogels.

A detailed discussion of the other distinctive features of the mesogels is beyond the scope of these article. The main characteristics, focusing on the case of lamellar mesogels, are as follows: (1) The extension and compression behaviour are asymmetric. The extension is dominated by the elasticity of the bridging chains. In marked contrast, the compression is opposed by the osmotic pressure due to both bridging and non-bridging chains. (2) The deformation of the B chains is non-affine. (3) Since the lamellar mesogel is not isotropic, the Young and shear moduli are not simply proportional to each other. (4) The extension of lamellar mesogels in a poor solvent exhibits a novel force law. For certain regimes the stress is independent of the strain.[30] This is the signature of a first-order phase transition involving the coexistence of a dense phase of weakly deformed chains and a dilute phase of strongly stretched ones.

IV. POLYELECTROLYTE MESOGELS

The behaviour of the swollen mesogels is modified when the B blocks are polyelectrolytes. As in the case of mesogels with neutral B blocks, the analysis is closely related to that of a free brush. Two extra contributions come into play when a polyelectrolyte brush is immersed in a solvent of high dielectric constant, thus promoting dissociation.[31] One is the mixing entropy of the mobile counterions. The second is the electrostatic energy between the charged brush and the oppositely charged counterions. This last term appears only when the counterion cloud extends beyond the boundary of the brush, thus causing local deviations from electroneutrality. Typically, this contribution is important in the discussion of free, dilute micelles and cylinders or of sparsely grafted planar brushes. In our case, this effect may be neglected because of symmetry, i.e., each brush is surrounded by identical brushes, thus enforcing symmetry with respect to the midplane and local electroneutrality. Accordingly, the important term is due to the mixing entropy of the counterions. In principle, one must allow for the Debye-Hückel correction, allowing for correlations between the ions and the corresponding decrease of their entropy. This correction is, however, small and the important features of the system are obtained when the countertions are considered as an ideal gas. The corresponding term to the free energy density is of the form $\rho_{\text{ion}} \ln \rho_{\text{ion}}$. Because of the local electroneutrality, the volume fraction of the ions, ρ_{ion} is related to the monomer volume fraction as $\rho_{\text{ion}} = \phi(r)/m$ where m is the typical distance between neighbouring ionic groups along the chain in monomer units. The counterion mixing free energy per chain is, thus,

$$F_{\rm ion}/kT = (\Sigma/R^{d-1}a^3m)\int_R^{R+H}[\phi(r)\ln\phi(r)/m]r^{d-1}dr. \tag{15}$$

As in the previous section, the equilibrium state is found by minimising $F_{\rm chain}$ subject to the constraint of monomer conservation, Eq. (11). In the present case, there is an extra term in the free energy per chain and $F_{\rm chain} = F_{el} + F_{\rm int} + F_{\rm ion}$. The corresponding minimum condition is $-(R^{d-1}a/\Sigma)(\phi r^{d-1})^{-2} + (\Sigma/a^3R^{d-1})(v\phi + m^{-1}\phi\ln\phi/m + \lambda) = 0$. Under good solvent conditions the interaction terms are negligible and the scaling form of ϕ is given by $(R^{d-1}/\Sigma)^2a^4(\phi r^{d-1})^{-2} = m^{-1}\phi\ln\phi/m + \lambda = \Lambda^{-2}$. This leads to $\phi = \Lambda(R^{d-1}/\Sigma)a^2/r^{d-1}$ where $\Lambda = Na/H$ is a constant determined by Eq. (11). $F_{\rm chain}$ and H_{eq} are obtained by minimising $F_{\rm chain} = F_{el} + F_{\rm int}$ with respect to H. For $H \gg R$ the result is

$$H_{\rm eq} \approx aNm^{-1/2} \tag{16}$$

$$\phi \approx (R^{d-1}/\Sigma)a^2m^{1/2}/r^{d-1}. \tag{17}$$

and

$$\langle\phi\rangle \approx (a^3R^{d-1}/\Sigma)m^{d/2}N^{1-d}. \tag{18}$$

As opposed to the neutral mesogel, te equilibrium H_{eq} exhibits the same scaling behaviour for all three geometries and for both good and θ solvents. This is because the stretching of the brush is due to the osmotic pressure of the counterions, $\pi \approx kT\langle\phi\rangle/m$, rather than to monomer-monomer interactions. In turn, the osmotic force per chain is roughly $f_{\rm os} \approx \pi\Sigma H^{d-1}/R^{d-1}$ and since $\langle\phi\rangle \approx (R^{d-1}/\Sigma)Na^3/H^d$, it scales as $f_{\rm os} \approx kTN/H$ for all the situations noted above. Balancing $f_{\rm os}$ against the elastic restoring force per chain $f_{el} \approx kTH/Na^2$ yields the equilibrium value of H as listed above.

The behaviour of polyelectrolyte mesogels reduces to that of neutral mesogels when m is increased, *i.e.*, for weakly charged mesogel. Such is also the case upon addition of salt. The rough characteristics of polyelectrolyte mesogels are rather similar to those of neutral mesogels as listed at the conclusion of section III. However, the collapse of a polyelectrolyte mesogel takes place as a first-order phase transition. Finally, the stretching behaviour of such mesogels in poor solvent has not yet been studied.

V. LIQUID CRYSTALLINE MESOGELS

Liquid crystalline mesogels are predicted to exhibit a number of novel features involving electromechanical, electro-optic and mechano-optic effects.[9,10] The simplest system of this type is a lamellar mesogel with main chain LCP B blocks which is swollen by a nematic solvent. Another essential ingredient is the proper choice of the A blocks so that the glassy A domains impose a perpendicular orientation on the nematic director, **n**, at the interface (so called homeotropic anchoring.[32]) Our discussion of this system is entirely qualitative, focusing on the simplified elementary unit of the mesogel, *i.e.*, a doubly-anchored nematic brush consisting solely of bridging LCPs ($q = 1$). This brush is swollen by a θ nematic solvent chemically identical to the mesogenic monomers incorporated into the backbone of the LCP. In this case, repulsive monomer-monomer interactions do not play a role and the LCPs retain, essentially, their melt configurations. The swelling of the mesogel is due to repulsive ternary interactions between the monomers. Due to the imposed anchoring conditions, the spacing between the A layers is equal to $R_{\|_o}$ of a LCP in a θ nematic solvent. The swelling behaviour of the mesogel is not very distinctive. The novelty is in the response of the system to shear and to electric fields.

To appreciate these features, it is helpful to summarise the behaviour of a monomeric nematic in a slit imposing homeotropic anchoring.[33] Two features are of interest: (1) Monomeric nematics respond to shear as simple fluids in the sense that there is no elastic response, *i.e.*, the shear modulus is zero. The so-called Franck elasticity of the nematics is due to the distortion of the director field and does not respond to strains. Thus, qausi-static shear of the two plates causes no nematic distortion even though fast displacement does. (2) A nematic can be aligned by an electric field because of its electric anisotropy, $\Delta\varepsilon$. If $\Delta\varepsilon > 0$ the nematic director tends to align with the field. When such a nematic is confined to a slit imposing homeotropic anchoring and subjected to a field, E, parallel to the confining plates, a Fréedericksz transition takes place: There is no distortion of the director field while $E < E_c = (\pi/H)(k/\Delta\varepsilon)^{1/2}$ where k is the relevant nematic elastic constant. In this regime, the effect of the anchoring is dominant throughout the slit and the director field is perpendicular to the plates. When $E \gg E_c$ the nematic at the interface still obeys the anchoring conditions but $\mathbf{n}$ at intermediate orientations is aligned with the field. The onset of the nematic distortion, at $E = E_c$, has the features of a second-order phase transition named after Fréedericksz. For the reasons listed in (1) above, the transition is not associated with strain or stress of the two confining plates.

Both (1) and (2) are modified in our system because the two plates are now bridged by LCP which are, in turn, coupled to the director field of the nematic solvent. In particular: (i) Shear strain of the two plates now causes a nematic distortion since it induces a tilt of the bridging LCP. The onset of this distortion is continuous and no phase transition is involved. Remarkably, at certain regimes the shear modulus is dominated by the Franck elasticity of the nematic solvent. (ii) The onset of the Fréedericksz transition is shifted to higher fields because of the effect of the elasticity of the bridging chains. (iii) The Fréedericksz transition now gives rise to shear strain of the confining plates because of the LPC-mediated coupling to the nematic distortion. (iv) The shear modulus of the brush vanishes as E approaches E_c from below because of the diverging susceptibility of a system undergoing a second order phase transition.

VI. OLD EXPERIMENTS AND NEW SIMULATIONS

Polycrystalline, multi-domain mesogels were observed in the mid 1960s by Skoulious *et al.*[34] and by Franta *et al.*[35] ABA triblock copolymers in a selective solvent formed birefringent physical gels. The cross-linking involved crystalline A domains. The nature of the mesogel, be it lamellar, cylindrical or micellar, was determined by the concentration of the copolymer. However, apart from their birefringence, these systems are essentially isotropic because of their polycrystalinity. Monocrystalline, aligned mesogels were observed in the mid 1970s by Folkes *et al.*[14] These experiments pioneered the procedure described in the Introduction, *i.e.*, shear alignment of an ABA melt in the appropriate mesophase followed by quenching to below $T_g(A)$ and swelling with a selective solvent. Anisotropic swelling was observed for lamellar and cylindrical mesogels. However, extensive swelling caused breakage of the glassy A domains. Beyond this point the gels lost their mesomorphic character and behaved as isotropic gels. Regrettably, this seminal study focused mainly on the shear alignment of the mesophase and overlooked the relationship to the polymer physics of networks.

Simulations of bridging of two surfaces by telechelic chains were recently carried out by Misra *et al.*[36,37] These simulations are, however, concerned with dilute systems and low adsorption energies, for which the relaxation times are short. Hopefully, these studies will be extended in the future to the regimes of direct relevance to the mesonetwork/mesogel problem, *i.e.*, high densities and high adsorption energies.

Acknowledgements

It is a pleasure to acknowledge helpful discussions with M. Matsen who also provided a copy of Reference 13 prior to publication.

References

1. (a) R. Fayt, R. Jerome and P. Teyssie, *J. Polym. Sci., Polym. Lett. Ed.*, **19**, 79 (1981); (b) C. R. Lindsay, D. R. Pau and J. W. Barlow, *J. Appl. Polym. Sci.*, **1**, 26 (1981); (c) R. Fayt, R. Jerome and P. Teyssie *J. Polym. Sci., Part B: Polym. Phys.*, **19**, 1269 (1981); (d) R. Fayt, R. Jerome and P. Teyssie *J. Polym. Sci., Part B: Polym. Phys.*, **20**, 2209 (1982); (e) Y. Lee and K. Char, *Macromolecules* **27**, 2603 (1994); (f) H. R. Brown, K. Char, V. R. Deline and P. F. Green, *Macromolecules*, **26**, 4155 (1993); (g) K. Char, H. R. Brown and V. R. Deline, *Macromolecules*, **26**, 4164 (1993).
2. (a) E. Pludman and N. Collins in *Adhesion Science and Technology*, L. H. Lee, Ed. (Plenum Press, New York, 1975) Vol. 9a; (b) W. F. Reichert and H. R. Brown, *Polymer*, **34**, 2289 (1993); (c) R. J. Chang and A. N. Gent, *J. Polym. Sci., Part B: Polym. Phys.*, **19**, 1619 (1981).
3. *Thermoplastic Elastomers*, N. R. Legge, G. Holden and H. Schroeder, Eds. (Hanser, Munich, 1987).
4. A. Halperin and E. B. Zhulina, *Europhys. Lett.*, **16**, 337 (1991).
5. A. Halperin and E. B. Zhulina. *Prog. Colloid Polym. Sci.*, **90**, 156 (1992).
6. E. B. Zhulina and A. Halperin, *Macromolecules*, **25**, 5730 (1992).
7. E. B. Zhulina, *Macromolecules*, **26**, 6273 (1993).
8. S. Misra and S. Varanasi, *Macromolecules*, **26**, 4184 (1993).
9. A. Halperin and D. R. M. Williams, *Macromolecules*, **26**, 6652 (1993).
10. A. Halperin and D. R. M. Williams, *Phys. Rev. E*, **49**, R986 (1994).
11. A. N. Semenov and A. V. Subotin, *Sov. Phys. JETP*, **74**, 660 (1992).
12. S. T. Milner and T. A. Witten, *Macromolecules*, **25**, 5495 (1992).
13. M. Matsen, *J. Chem. Phys.* (in press).
14. (a) M. J. Folkes, A. Keller and J. A. Odell, *J. Polym. Sci., Polym. Phys. Ed.*, **14**, 833 (1976) and *ibid.*, **14**, 847 (1976); (b) A. Keller and J. A. Odell in *Processing, Structure and Properties of Block Copolymers*, J. M. Folkes, Ed (Elsevier, New York, 1985).
15. F. S. Bates and G. H. Fredrickson, *Annu. Rev. Phys. Chem.*, **21**, 525 (1990).
16. A. Halperin, M. Tirrell and T. P. Lodge, *Adv. Polym. Sci.*, **100**, 31 (1992).
17. A. N. Semenov, *Sov. Phys. JETP*, **61**, 733 (1985).
18. A. Alexander, *J. Phys. France*, **38**, 977 (1977).
19. A. Johner and J. F. Joanny, *Europhys. Lett.*, **15**, 265 (1991).
20. E. B. Zhulina and T. Pakula, *Macromolecules*, **25**, 754 (1992).
21. The discussion follows A. Halperin and D. R. M. Williams, *Faraday Discuss.*, **98**, 349 (1994).
22. (a) T. Odijk, *Macromolecules*, **19**, 2313 (1986); (b) A. R. Kokhlov and A. N. Semenov, *Sov. Phys. Usp.*, **31**, 988 (1988); (c) G. T. Vroege and H. N. W. Lekkerkerker, *Rep. Prog. Phys.*, **55**, 124 (1992); (d) P. G. deGennes in *Polymer Liquid Crystals*, A. Ciferri, W. R. Krigbaum and R. Meyer, Eds. (Academic

Press, New York, 1992); (e) M. Warner in *Side Chain Liquid Crystalline Polymers*, C. B. McArdle, Ed. (Chapman and Hall, New York, 1989).
23. H. Yamakawa, *Modern Theory of Polymer Solutions* (Harper and Row, New York, 1971).
24. A. Halperin and D. R. M. Williams, *Europhys. Lett.*, **21**, 575 (1993) and D. R. M. Williams and A. Halperin, *Macromolecules*, **26**, 4208 (1993).
25. A. Halperin and D. R. M. Williams, *Europhys. Lett.*, **20**, 601 (1992).
26. D. R. M. Williams and A. Halperin, *Europhys. Lett.*, **19**, 693 (1992) and *Macromolecules*, **26**, 2025 (1993).
27. P. G. deGennes, *Scaling Concepts in Polymer Physics* (Cornell University Press, Ithaca, N.Y. 1979).
28. M. Daoud and J. P. Cotton, *J. Phys. France*, **43**, 531 (1982).
29. E. B. Zhulina, O. V. Borisov, V. A. Priamitsyn and T. M. Birshtein, *Macromolecules*, **24**, 140 (1991).
30. A. Halperin and E. B. Zhulina, *Macromolecules*, **24**, 5393 (1991).
31. (a) P. Pincus, *Macromolecules*, **24**, 2912 (1991); (b) R. S. Ross and P. Pincus, *Macromolecules*, **25**, 2177 (1992); (c) S. Misra, S. Varanasi and P. P. Varanasi, *Macromolecules*, **22**, 4173 (1989); (d) J. Wittmer and J. F. Joanny, *Macromolecules*, **26**, 2691 (1993); (e) O. V. Borisov, E. B. Zhulina and T. M. Birshtein, *Macromolecules*, **27**, 4795 (1994); (f) S. J. Miklavic and S. Marcelja, *J. Phys. Chem.*, **92**, 6718 (1988).
32. B. Jerome, *Rep. Prog. Phys.*, **54**, 391 (1991).
33. (a) P. G. DeGennes and J. Prost, *The Physics of Liquid Crystals*, 2nd. ed. (Clarendon Press, Oxford, 1993); (b) S. Chandrasekhar, *Liquid Crystals* (Cambridge University Press, Cambridge, 1992).
34. A. Skoulious, G. Tsouladze and E. Franta, *J. Polym. Sci.*, **64**, 507 (1963).
35. E. Franta, A. Skoulious, P. Rempp and H. Benoit, *Makromol. Chem.*, **87**, 271 (1965).
36. S. Misra and W. L. Mattice, *Macromolecules*, **27**, 2058 (1994).
37. S. Misra, M. Nguyenmisra and W. L. Mattice, *Macromolecules*, **27**, 5037 (1994).